International Journal of Geo-Information

MDPI

Article

Wildfire Risk Assessment Based on Geospatial Open Data: Application on Chios, Greece

Nektaria Adaktylou [1], Dimitris Stratoulias [2,3,*] and Rick Landenberger [1]

[1] Department of Geology and Geography, Eberly College of Arts & Sciences, West Virginia University, Brooks Hall, 98 Beechurst Avenue, Morgantown, WV 26505, USA; nektaria.adaktylou@mail.wvu.edu (N.A.); Rick.Landenberger@mail.wvu.edu (R.L.)

[2] Informetrics Research Group, Ton Duc Thang University, Ho Chi Minh City 758307, Vietnam

[3] Faculty of Applied Sciences, Ton Duc Thang University, Ho Chi Minh City 758307, Vietnam

* Correspondence: dimitris.stratoulias@tdtu.edu.vn

Received: 15 July 2020; Accepted: 21 August 2020; Published: 28 August 2020

Abstract: Wildfires burn tens of thousands of hectares of forest, chaparral and grassland in Mediterranean countries every year, giving rise to landscape, ecologic, economic, and public safety concerns. On the Greek island of Chios and in many other Mediterranean landscapes, areas affected by fire are difficult to access and control due to rugged terrain, requiring wildfire preparedness and response plans that support fire fighting. This study utilized open source data and a weighted linear combination to extract factors that determine wildfire risk. Landsat satellite imagery and publicly available geospatial data were used to create a Geographic Information System and a multi-criteria analysis to develop a methodology for spatially modeling fire risk on Chios, a Greek island with frequent fire occurrence. This study focused on the static, structural component of the risk assessment to produce a spatial distribution of fire risk as a thematic map. Fire weather conditions were accounted for using Fuel Moisture Content, which reflected dryness of dead fuels and water deficit of live biomass. To assess the results, historic fire data representing actual occurrence of fire incidents were compared with probable fire locations predicted by our GIS model. It was found that there was a good agreement between the ground reference data and the results of the created fire risk model. The findings will help fire authorities identify areas of high risk for wildfire and plan the allocation of resources accordingly. This is because the outputs of the designed fire risk model are not complex or challenging to use in Chios, Greece and other landscapes.

Keywords: fire risk; forest management; GIS; geospatial data; remote sensing; multiple-criteria decision analysis

1. Introduction

Forests, shrublands and other wildlands serve paramount ecological and environmental functions and play a vital role in human welfare [1]. It is widely recognized that they can regulate rainfall, moderate temperature, reduce soil erosion, and cycle atmospheric carbon [2–4]. They also provide a great variety of outdoor recreation opportunities and connect people with nature in a diversity of settings and activities.

Wildfires have a significant impact on the physical and biological environment; they affect land use and land cover, ecosystems, biodiversity, and climate change. As such, they influence the socio-economic system of the areas where they occur. The Mediterranean region is a prime example of an extensive area where human-induced fires prevail and naturally-occurring fires are infrequent. Natural causes represent from 1–5% of all ignitions, depending on the country, probably due to the absence of climatic phenomena such as dry lightning storms [5]. Recent studies in the USA have also

shown that human activities have created a spatial and seasonal "fire niche", accounting for 84% of all wildfires and 44% of the total area burned [6]. Human-induced fires are attributed to land conversion, timber harvesting, slash-and-burn agriculture, conflicts over property ownership and land use rights, negligence, and arson [7].

Mediterranean-type ecosystems are among the most diverse areas in the world due to the range of climate conditions that provide a wide variety of habitats for various species. At the same time, the Mediterranean climate is characterized by prolonged hot and dry summers that favor fire ignition. Consequently, native vegetation (mostly pine trees and spiny evergreen shrubs) has adapted to periodic wildfires [8]. However, this fire adaptation in the Mediterranean basin specifically has not been the main driving factor for speciation [9]. The average annual number of wildfires in undeveloped areas throughout the Mediterranean basin has increased significantly in the past 50 years. Other studies have shown that in Spain, Portugal, Italy, and Greece, the average total burnt area has quadrupled from the 60's until the present [10]. Moreover, the projection of the yearly average burnt area in the Mediterranean region is predicted to increase by approximately 150–220% by 2090 relative to 2000 [11].

Some Mediterranean areas are experiencing prolonged drought periods with high temperatures and strong local winds that affect the frequency and the intensity of their fires. The Mediterranean type of vegetation itself has chemical, physical and physiological properties that increase its flammability with age [12]. A large part of the Mediterranean basin is a semi-natural landscape that has a long history of human impacts on forests and shrublands, and most of the fire outbreaks have been a result of human activities [13].

All fire-prone countries have some form of fire risk assessment and oftentimes more than one (various indices). Studies have shown that vegetation and topography have been widely recognized as the dominant controls on fire severity in many types of forest and shrubland ecosystems [14–18]. Fire 'risk' is a term used for the probability that a fire might start in a certain area, affected by the nature and incidence of causative agents [19,20]. Due to the complex nature of forest and shrubland, maps showing fire risk and fire danger can be particularly challenging to produce [11]. In Mediterranean ecosystems specifically, difficulties in measurement and quantification of important factors related to fire risk and danger often lead to either a descriptive approach to the problem or a total exclusion from forest management planning [19].

Several approaches have been suggested for modeling potential fire occurrence, such as linear regression and logistic regression analysis [21], algorithms based on normalized brightness and wetness indices (FIRA), artificial neural networks [22,23], and statistical approaches [24]. Numerous research projects have developed wildfire risk models for specific regions based on physiographic and environmental factors that influence wildfire [7,25,26]. Fire risk assessment usually takes different forms depending on the objectives for which the assessments are made. In Europe, the European Commission Services deals with a multitude of forest fire risk and danger approaches in the various member states. Consequently, the Joint Research Centre (JRC) of the European Commission created the European Forest Fire Information System (EFFIS) that provides reliable and up-to-date information on forest fires in Europe. The dynamic aspect of this model is defined primarily by weather; for example, drought is an important factor that often creates favorable conditions for the ignition and propagation of fire. Conversely, increased rainfall and humidity reduces the probability of ignition.

In-Situ meteorological data are usually collected at a low spatial resolution, which is inconsistent with the fine scale at which site-level fire severity is assessed and predicted. Spatially interpolated data from weather stations can partially mitigate this issue, but in regions where weather stations are sparse, this technique is inadequate. The lack of credible and timely weather data limits the understanding of spatial controls on fire-specific events.

Several methods using fire weather conditions have been proposed for fire risk applications. The most common are field measurements [27], the use of calibrated sticks and the computation of meteorological indices [28]. Fire weather conditions are often characterized using the metric of Fuel Moisture Content (FMC), which reflects dryness of dead fuels and water deficit of live biomass [29].

Air temperature influences the temperature of the fuel and therefore the quantity of heat energy required to raise it to its ignition point. Relative humidity is highly correlated with fuel moisture and therefore plays an important role in controlling fuel flammability, particularly of fine fuels [30]. However, none of the methods using FMC are completely satisfactory [31].

Remotely sensed data allows the acquisition of information of the factors that determine fire risk, such as topography, vegetation, weather, and other parameters at considerably finer temporal and spatial resolutions. This alleviates the need for costly and intensive fieldwork and interpolation methods that link the data directly to vegetation dynamic processes [32]. Advances in remote sensing allow examination of fine-scale fire weather effects on fire severity. For example, an approach for the remote sensing of FMC has been to estimate the change in canopy water content over time, using a liquid-water spectral index, such as the Normalized Difference Infrared Index (NDII). NDII is based on the ratio of the near-infrared and short-wave infrared reflectance bands (1.65 μm). It is a robust indicator of water availability in the soil for use by vegetation [33]. This index is based on reflectance measurements sensitive to changes in water content of plant canopies. The NDII uses a normalized difference formulation instead of a simple ratio, and its value increases with increasing water content [34].

In Greece, the Forestry Service has been using three classes for the static component of the risk assessment, based primarily on local fire history (number of fires and area burned) over a 30 year period. The General Secretariat of Civil protection provides a daily fire danger prediction map for the entire country. The map is produced by a team of forest fire experts and meteorologists and is published once a day around 13:00pm and is valid for the next day. An example of this map is shown in Figure 1. As can been seen, the spatial resolution of the product is coarse, providing a fire danger prediction class at the provincial level. For example, Chios, the study area examined here, is assigned a single class for the entire island.

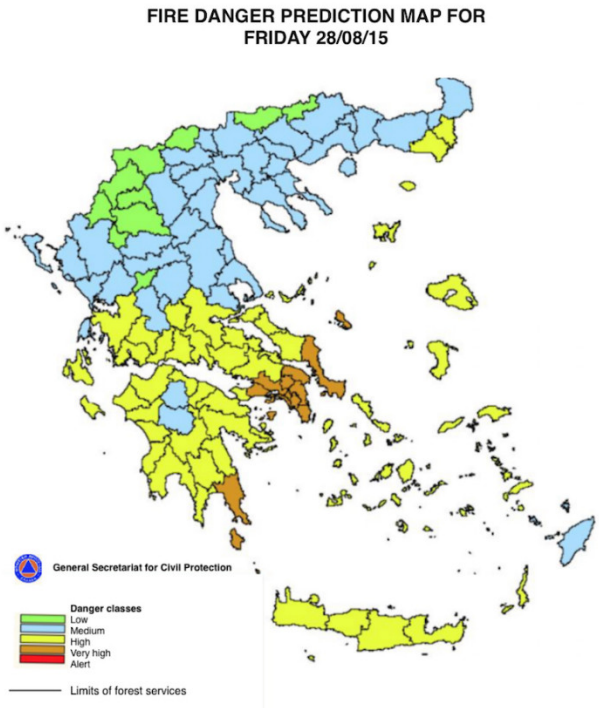

Figure 1. Daily fire prediction map at national scale for the day 28 August 2015. A class for fire danger prediction is assigned for each province of the country.

Several studies have attempted to create a multi-criteria evaluation based on remote sensing data and GIS techniques [7,26,35–42]. However, there is a need to establish the basic factors that affect the wildfire spread in our study area Chios such as fuel, fire behavior and human intervention (fire-fighting

effectiveness) [43,44]. It is also important to examine how environmental parameters (vegetation cover (V), slope (S), aspect (A), elevation (E), illumination (I)) drive fire propagation. This will help understand how the most important environmental parameters, such as vegetation cover/fuel type and FMC, drive fire propagation in Chios. Natural ignitions in Chios are extremely rare because of the lack of dry lightning or other natural ignition source. However there is need to understand how fire ignition correlates with human factors (be it negligence or arson), including access to roads and proximity to human settlements. These are important factors in wildfire management in Chios because they indicate human access and activity that can lead to ignition [45,46]. Settlements in Chios simply represent human presence, while roads provide relatively easy access to undeveloped forest and shrubland.

The goal of this work was to design and create a decision support system to assist fire prevention and management on the island of Chios. The current study aimed to produce an easy-to-use tool for the estimation of fire risk using free data and open source software. It showcases the usability of public domain geospatial data for information extraction with a methodology that can be transferable to other landscapes and a final product that can be made available freely to the public.

2. Materials and Methods

2.1. Study Area

The study area is the island of Chios (Figure 2), that is located in the Northeastern Aegean Sea in Greece. Chios is the fifth largest island in the Aegean, covering a total area of 902 km^2 and a coastline of 213 km. The total population is 54,000 inhabitants from which approximately half are residing in the capital Chora. Chios is an island of significant ecological importance; it became internationally known during the 13th century due to the production of the Chios mastic, the resin of the mastic tree (*Pistacia lentiscus* L. var. *chia* (Desf. ex Poiret) DC.) in 21 villages. Many beneficial properties and uses have been attributed to the Chios mastic since antiquity [47]. Mastic trees grow, among other sclerophyllous species consisting the main vegetation type in Aegean islands [48], in the south part of the island, an area which has been affected dramatically by recent severe fire events.

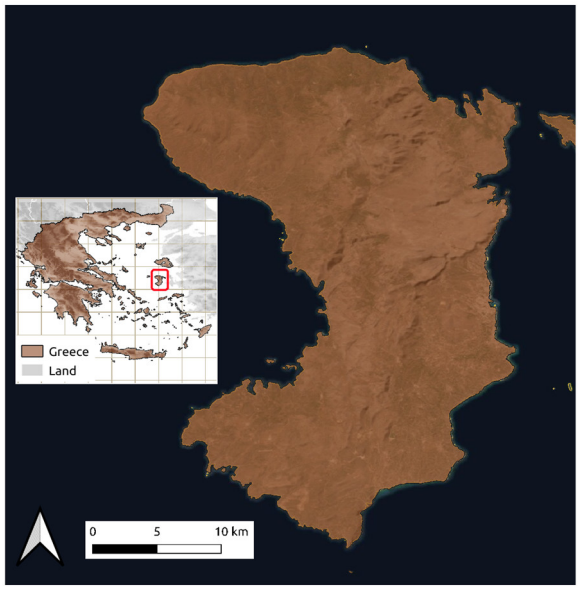

Figure 2. The study area, island of Chios, and its relative location to Greece (inset).

Moreover, the island has five areas that are part of the NATURA 2000 Networking Program, an initiative which ensures the long-term survival of Europe's most valuable and threatened species and habitats [49]. Two of these areas are 'Sites of Community Importance' (SCI) according to the

Directive 92/43/EEC (habitats) and three are 'Special Protection Areas (SPA) according to the Directive 2009/147/EU (birds).

The island's climate is warm and moderate (Temperate, Mediterranean (Csa)) with modest variation due to the stabilizing effect of the surrounding sea. The island normally experiences steady breezes (average 10.8–18 km/h) throughout the year, with a dominant northerly or southwesterly wind. Mediterranean-type climate regions are dominated by evergreen sclerophyllous-leaved shrublands, semi-deciduous scrub, and woodlands, all of which are prone to widespread crown fires [50]. A warmer and drier climate can affect wildfire activity by leading to more favorable conditions for burning and also by modifying the structure of the fuel available to be burned [51]. The typical pattern is a relatively wet and cool season in winter that spurs plant growth, followed by a dry and hot summer season (Figure 3) in which the new vegetation withers and becomes flammable tinder. There is a negative correlation between temperature and precipitation, which means that warmer than normal temperatures usually result in drier than normal conditions and colder periods are likely to be wetter. As it can be seen in Figure 3, based on 30-year data available for the island, the temperatures are the highest for the period between July and August while the precipitation is the lowest, resulting in an ideal scenario for wildfire. This agrees with the existing records of fires on the island that have occurred in that 30-year time period.

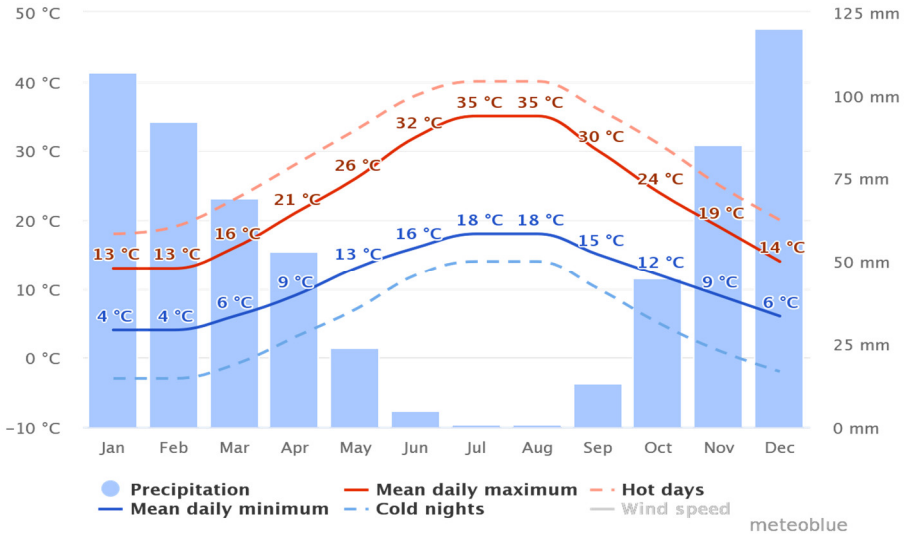

Figure 3. Annual fluctuation of temperature and rainfall in the island of Chios. The solid red line shows the maximum temperature for an average day for every month on Chios; the solid blue line shows the average minimum temperature; the dashed red and blue lines show the average of the hottest day and coldest night of each month for the last 30 years. The period between June and September is dominated by hot and dry conditions, ideal for the ignition and propagation of fires (Source: meteoblue).

Seasonal climate and recent weather conditions also shape FMC, the key factor determining how readily fuels burn. While live plants and trees can hold as much as three times their weight in moisture during a healthy growing season, dead fuels hold far less moisture, topping out at about 30%. Furthermore, moisture levels of dead fuels can fluctuate daily [52]. Chios is one of the most fire-prone areas in Greece with a total burnt area for the period 1993–2005 of 30,255 ha, the result of 446 recorded fires and a mean burned area per incident estimated at 67.8 ha. In July 2007, fires occurred in the north part of the island while in 2012 the most devastating fire of the past 30 years burned more than 14,800 ha. Extensive fires also occurred in the summer of 2016 at the regions of Plata (23th July) and Sidirounta (26th August), burning 4,343 and 622 ha respectively (Figure 4).

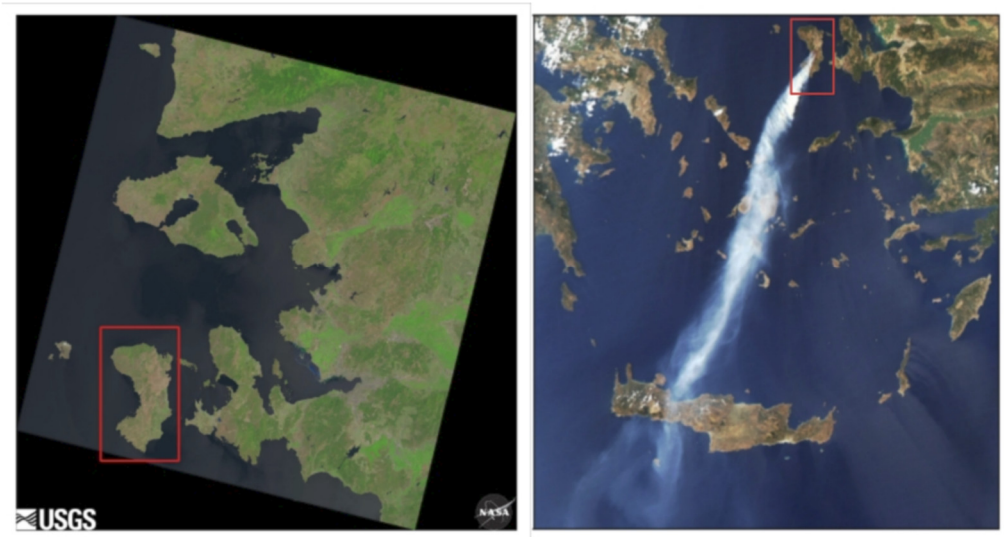

(**a**) (**b**)

Figure 4. The study area in a Landsat-8 scene acquired on 13 July 2016 used in this study and the area of interest in the bounding box (**a**); the smoke plume dispersing over the Aegean sea from a historic fire that occurred in on Chios captured by the MODIS sensor on NASA's AQUA satellite Aqua on 18th August 2012 (**b**).

2.2. Data

The present study is based on open access and freely available earth observation products and algorithms. Data from the Landsat 5, Landsat-7 ETM+ and Landsat-8 OLI satellite sensors, the Shuttle Radar Topography Mission (SRTM) Digital Elevation Model (DEM), the Corine Land Cover (CLC) 2012 (v.18.5.1) and the OpenStreetMap (OSM) were used to derive the fire risk map and the associated burn scars from three past fire seasons (2007, 2012 and 2016). CLC was retrieved in GeoTIFF raster format at 100 m spatial resolution from the Copernicus Land Monitoring Service.

The SRTM DEM was used for the extraction of the physiographic attributes (i.e., slope, aspect, and elevation) and illumination. A visual investigation of the Advanced Land Observing Satellite (ALOS) DEM provided by JAXA and the SRTM DEM provided by NASA, both at a resolution of 1 arc-second (30 m), revealed that these two datasets are very similar in the area of study; the SRTM DEM was eventually selected, as it is not affected by cloud cover. Two 1 arc-second global SRTM tiles cumulatively covering the region of interest (38 North/25 East and 38 North/26 East) were downloaded in GeoTIFF format from the EarthExplorer website. They were then co-registered, subsetted to the area of interest (AOI), spatially resampled to a 30 m × 30 m grid to approximate the Landsat-8 spatial resolution, and projected on the latter's coordinate system (WGS 84/UTM zone 35N).

Three pairs of Landsat images were used to map the footprint of the three fire events to investigate the robustness of the methodology proposed at the local scale. The burn scar from the fire occurring in the middle of July 2007 in the north part of the island was extracted from a pair of Landsat-5 TM images acquired on 05 July 2007 at 08:46 and 28 July 2007 at 08:52. The fire of 2012 was estimated from a pair of Landsat-7 ETM+ images acquired on 10 July 2012 at 08:47 and 15 November 2012 at 08:48. The largest fire that occurred in July 2016 was mapped with pre- and post-fire Landsat-8 OLI scenes acquired on 13 July 2016 at 08:52 and 29 July 2016 at 08:52 respectively. The cloud cover of the whole scene is less than 1% with no apparent haze over any of the images and the entire island of Chios is covered with a single Landsat image (Path 181, Row 33). All Landsat data were downloaded from the Earth Resources Observation and Science Center (EROS) of the U.S. Geological Survey (USGS) at level-1 standard processing level.

2.3. Methodology

The flowchart to derive the parameters related to fire risk assessment is presented in Figure 5. The CLC 2012 dataset was used to derive the LULC layer, the SRTM DEM data was used to derive the slope, elevation and illumination layers, and the OSM data was used to derive the proximity to road layer. Human settlement proximity was estimated from a vector layer built by taking into consideration the OSM map and the 2011 population-housing Census published from the Hellenic Statistical Authority [53]. The resulting factors were categorized in five levels from one to five (LULC from zero to four) according to the thresholds presented in Table 1. Finally, each of these five layers was assigned a weight and then analyzed and combined to produce the final result. The Landsat scene pairs were used for the extraction of the burned area as the aftermath of the three large fire incidents, as well as the NDII spectral index. The processing was performed in GDAL, Bash and R programming languages, and the maps were created using QGIS. The software and data used are in the open access domain, which makes the implementation of the proposed methodology readily available and without any cost for software or data. The derivation of each layer is described in detail in the following paragraphs.

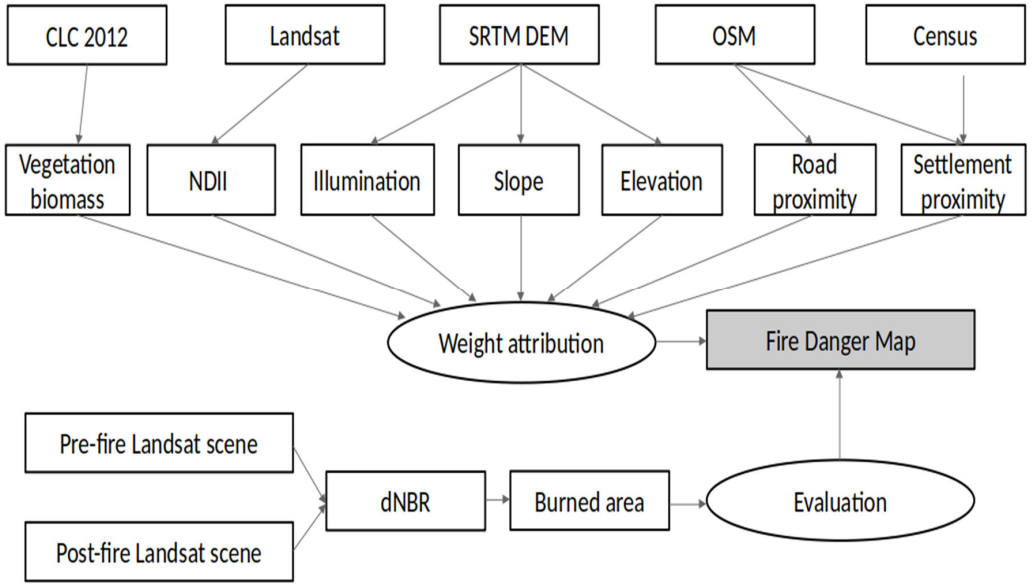

Figure 5. The flowchart of the work progress. Landsat-5/7/8 images were used for each one of the three fire incidents investigated in the current study and the flowchart, other than the use of a different Landsat image, which was identical for each case.

Table 1. Factors and categorical values used in the model.

Categorical Value	LULC	NDII	Illumination	Slope (Degrees)	Proximity to Roads (m)	Proximity to Settlements (m)	Elevation (m)
Very low	According to next table (0)	>0.008	<1,546,000	<5	>1600	>3200	>760
Low	According to next table (1)	0.006–0.008	1,546,000–1,612,000	5–10	800–1600	1600–3200	570–760
Medium	According to next table (2)	0.004–0.006	1,612,000–1,678,000	10–15	400–800	800–1600	380–570
High	According to next table (3)	0.002–0.004	1,678,000–1,744,000	15–25	100–400	200–800	190–380
Very high	According to next table (4)	<0.002	>1,744,000	>25	<100	<200	<190

2.3.1. Vegetation—Land Use/Land Cover

The amount of fuel available for combustion was derived from the CLC 2012 dataset. The classes identified on Chios were reclassified in integer numbers from zero to four (Table S1) based on the land cover type and taking into consideration the possibility of fire ignition for each land cover type.

For example, rice fields and similar irrigated areas were assigned a low score, since, although they are representing vegetation with considerable vegetation biomass, the permanent water table makes these areas unlikely for the ignition or the propagation of a fire. Olive groves, fruit trees, and berry plantations, despite having high content in biomass, are assigned a lower score value (i.e., 2) in comparison to non-irrigated trees as suggested in the existing literature [54].

2.3.2. NDII

The NDII index (Equation (1)) is a reflectance measurement that is sensitive to changes in water content of plant canopies and plant roots. In the present study, the index is used as a proxy for FMC.

$$\text{NDII} = (\rho_{819} - \rho_{1649})/(\rho_{819} + \rho_{1649}) \quad (1)$$

where ρ is the spectral reflectance at 1649 and 819 nm, the shortwave infrared and near infrared bands, respectively. Throughout the range beyond 1.3 μm, leaf reflectance is approximately inversely related to the total water present in a leaf, a function of the moisture content. In the range from about 0.7 to 1.3 μm, a plant leaf typically reflects 40–50% of the energy incident upon it primarily due to the internal structure of plant leaves [55].

The NDII index was first assessed for different years after 2006, at different dates of the July–August period, and an emerging repetitive pattern was identified for the island (except for the areas burned in 2007, 2012, and 2016). Thus, four cloud free images during the summer of 2006 (2 July, 17 July, 19 August and 4 September), before the major fire events, were chosen to derive the NDII, and the average value of the four was used as the representative NDII layer.

2.3.3. Topography

Since temperature has a constant lapse rate and oxygen levels are reduced with height, elevation and the fire occurrence are inversely related. The DEM was used for elevation values and was reclassified in five classes (in 190 m increments). High values (corresponding to high altitudes) were attributed to the lowest risk class value. Slope directly influences moisture levels, as steeper slopes are subject to higher water runoff rates compared to shallow slopes, and rugged topography is generally more exposed to direct sunlight (illumination), which leads to drier vegetation. Moreover, steep topography plays a role in the formation of local winds and allows fire to spread more quickly up slopes. Slope was derived from the DEM, and the values were aggregated in groups according to FFTAICP and were given the weight factor presented in Table 1.

2.3.4. Illumination

Illumination is a measure of how much direct sunlight is received by a surface, based on its angle and aspect. It is calculated based on a mathematical model that provides the amount of sunlight that strikes any point on Earth's surface during a given day. Illumination directly relates to surface temperature and therefore to the moisture of fuels and the fire ignition risk factor. We followed the methodology proposed in [56]. For the derivation of illumination, the map coordinates of the center of the scene were used as presented in Table 2.

The apparent sunrise (05:03) and the apparent sunset (19:40) on 13 July 2016 were then estimated and the whole hours between the apparent sunrise and sunset were identified from 6:00 to 19:00 with one digit increment. The values of the azimuth and zenith angles for each whole hour interval were calculated for the latitude and longitude of the center of the scene as estimated above, (from the website "http://www.esrl.noaa.gov/gmd/grad/solcalc/" (Input data: Geographic coordinates of the center of the scene, 13th July 2016, offset to UTC: +2, Daylight saving time: NO). Finally, the solar radiation (illumination) was estimated (Table 3) based on Equation (2):

$$\text{Solar radiation} = 1365 \times \cos(\text{Z}) \times 0.84^{\sec(\text{Z})} \quad (2)$$

This formula yields the solar radiation dependent on the local time. For every whole hour of Table 3, the sun azimuth, sun elevation and the DEM are input in the hillshade function of QGIS. Therefore, the 14 rasters added up with the output from Equation (2) as the weight factor in the raster calculator to produce the illumination map. Thereafter, the illumination values of the raster layer were reclassified in five categories based on break points taken from the first standard deviation of the histogram and not in near-equal intervals, as in the case of slope, elevation and proximity to roads. Pixels with minor illumination values were assigned low class values (i.e., 1–2), while pixels with high illumination were assigned high values (i.e., 4–5).

Table 2. Map extent of the scene and coordinates of the center.

Map Scene Details	Coordinates (Decimal Degrees)	Coordinates (DMS)
Upper left	396149.405, 4273610.302	25d48′26.32′′ E, 38d36′17.72′′ N
Lower left	396149.405, 4221110.302	25d48′54.18′′ E, 38d 7′54.76′′ N
Upper right	428579.405, 4273610.302	26d10′46.97′′ E, 38d36′29.25′′ N
Lower right	428579.405, 4221110.302	26d11′ 6.14′′ E, 38d 8′ 6.09′′ N
Center	412364.405, 4247360.302	25d59′48.45′′ E, 38d22′12.50′′ N

Table 3. The values of the azimuth and elevation for whole hour equal intervals for the center of the chosen scene on 13 July 2016.

Local Time	Sun Azimuth	Zenith (Z)	Solar Radiation
6:00	69.51	80.64	76.158
7:00	77.98	69.41	292.635
8:00	86.54	57.79	524.575
9:00	96.11	46.06	736.849
10:00	108.41	34.59	908.933
11:00	127.59	24.18	1028.342
12:00	162.71	17.29	1086.067
13:00	208.94	18.55	1076.603
14:00	238.71	26.84	1001.416
15:00	255.34	37.68	866.16
16:00	266.62	49.28	681.24
17:00	275.79	61.01	462.022
18:00	284.25	72.57	228.822
19:00	292.8	83.63	31.476

2.3.5. Human Factor—Proximity to Roads and Settlements

While it is not possible to model human behavior (neglect, pyromania, etc.), the statistical approach developed by [57] shows a clear correlation between number of fire outbreaks and the proximity to a road or a settlement. Forested areas and activity centers (e.g., camping sites) provide easy access to the forest and influence the probability of ignition. In this study, the proximity to primary and secondary roads and populated settlements was chosen to represent the human factor. The thresholds selected for the road network proximity were 50 m, 200 m, 400 m, and 800 m.

2.3.6. Risk Factor Weight Attribution

The individual maps produced for all the factors examined (vegetation cover, NDII, illumination, slope, elevation, proximity to roads and settlements) are presented in Figure 6. A weighting factor was attributed to each one of the factors according to their relative significance on fire ignition and propagation. In most fire-related Multiple-Criteria Decision Analysis (MCDA), vegetation volume-related factors are considered the most important followed by the energy received (or temperature) and humidity. Gigović et al. [58] has compiled an assessment of the causative factors for fire spreading based on previous GIS MCDA studies and expert opinion and concluded that land use, topography, climate, and socioeconomics are the generic groups in sequence of importance in the context of forest fire spread. In the current study, the relative importance between factors was judged based on a meta-analysis. By considering findings from the literature review on this matter primarily, and secondarily taking into account the co-author's knowledge about the environmental and landscape conditions in Chios, the order of importance between the factors was established. Thereafter, the weight factor attribution is a critical step in an MCDA problem and several approaches have been developed such as the Analytical Hierarchy Process (AHP) [59], fuzzy inference system (FIS) [60] and compromise programming (CP) [61]. In the current study, we followed the pair-wise comparisons. The factor considered the most important was the LULC class as it is related to fuel available for combustion; the second factor considered was NDII since it relates to vegetation water content and consequently the humidity in the canopy, which is inversely related to fire ignition capacity. The third most important factor was illumination, which represents the solar radiation (and subsequently the solar energy available) per pixel. The slope factor follows, while human factors (i.e., road and settlement proximity) and elevation were given the lowest weights, sequentially. The numerical values of the weights were calculated according to the pair-wise comparison method (Table 4). In order to avoid the elimination of the weakest factor (i.e., elevation), which is a common problem for the pair-wise comparison technique, calculations of the diagonal of the table were taken into account as well. The final step of the process was to sum the seven raster layers using the calculated average and produce the fire risk map depicting the fire danger across the study area (Figure 7) based on Equation (3):

$$\begin{aligned}\text{Fire risk} = (0.25 \times \text{LULC}) + (0.21 \times \text{NDII}) + (0.18 \times \text{Illumination}) + (0.14 \times \text{Slope}) + \\ (0.11 \times \text{Road proximity}) + (0.07 \times \text{Settlement proximity}) + (0.04 \times \text{Elevation})\end{aligned} \quad (3)$$

Table 4. Pair-wise comparison of the fire risk factors for the extraction of the relevant weights.

Factor	LULC	NDII	Illumination	Slope	Road Proximity	Settlement Proximity	Elevation
LULC	V						
NDII	V	VI					
Illumination	V	VI	I				
Slope	V	VI	I	S			
Road proximity	V	VI	I	S	RP		
Settlement proximity	V	VI	I	S	RP	SP	
Elevation	V	VI	I	S	RP	SP	E
SUM	V = 7/28 = 0.25	VI = 6/28 = 0.21	I = 5/28 = 0.18	S = 4/28 = 0.14	RP = 3/28 = 0.11	SP = 2/28 = 0.07	E = 1/28 = 0.04

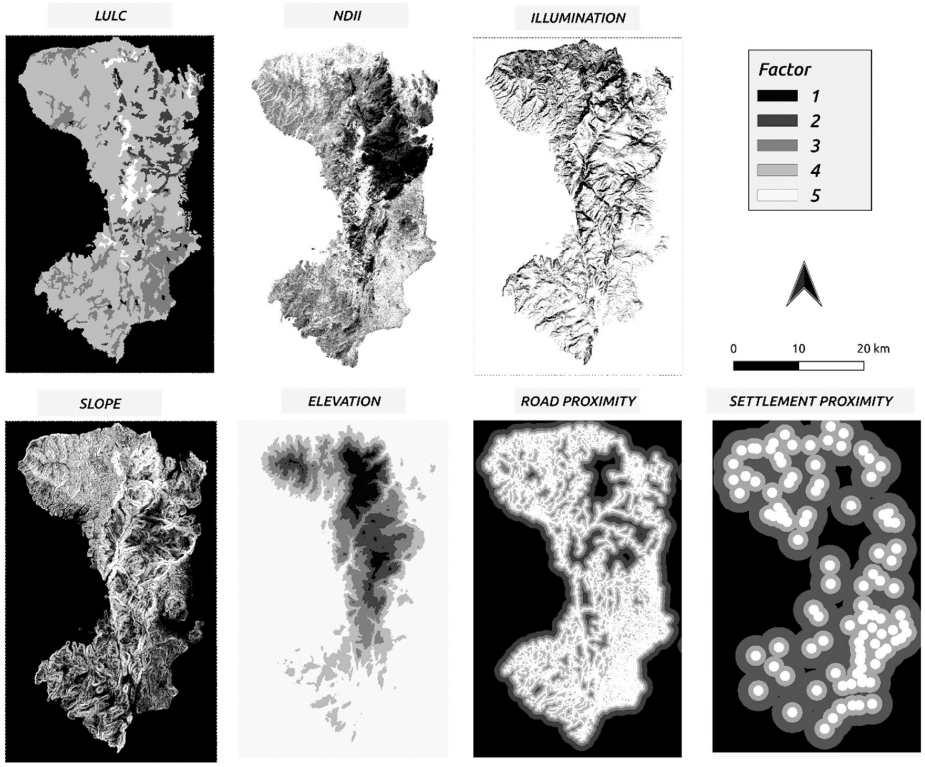

Figure 6. The results for all the individual factors examined in the fire risk model proposed.

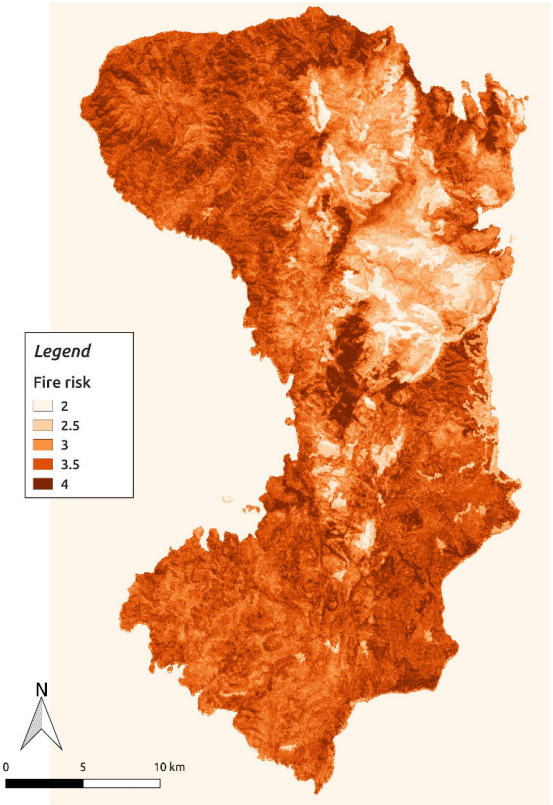

Figure 7. The fire risk map as a final product of the proposed approach. All the input layers were resampled to a 30 m × 30 m grid for the production of the map, equivalent to the 30 m spatial resolution of the Landsat satellite.

2.3.7. Burned Area Derivation

Optical satellite images were used to derive the burned area of three historic fire events that occurred during the summertime; a recent fire in 2016, the major fire on the island in the last 30 years, which occurred in 2012, and an older fire in 2007. Information about the Landsat optical images is given in the "Data" section. All images were first converted from Digital Numbers (DN) to top-of-atmosphere (TOA) reflectance according to Zanter [62] and based on Equation (4):

$$\rho_{\lambda'} = M_\rho \times Q_{cal} + A_\rho \quad (4)$$

where:

$\rho_{\lambda'}$ = TOA Planetary Spectral Reflectance, without correction for solar angle (unitless)
M_ρ = Reflectance multiplicative scaling factor for the band.
A_ρ = Reflectance additive scaling factor for the band (which is different for each satellite).
Q_{cal} = L1 pixel value in DN

The Landsat-7 images suffer from the scan line effect and the no-data values introduced in the images after May 2003 due to the failure of the Scan Line Corrector (SLC). To compensate for this data loss, the no-data pixels values were filled by interpolating the valid pixels at the edges of each void polygon.

Each pair of pre- and post-fire images was first used to derive the difference Normalized Burned Ratio (dNBR) index for each fire event. NBR was introduced by Key and Benson [63] and is derived from the algebraic combination of the formula in Equation (5):

$$NBR = (\text{near IR} - \text{middle IR})/(\text{near IR} + \text{middle IR}) \quad (5)$$

where dNBR is the difference of the NBR product of the two images; one taken before a fire incident (pre-fire) and one after (post-fire) as in Equation (6):

$$dNBR = (\text{pre-fire NBR}) - (\text{post-fire NBR}) \quad (6)$$

The dNBR was chosen as it has been successfully used in forest fire burn scar detection in Greece in past studies [64–67]. The pixels with values higher than 0.1 characterize burned areas. The map that was produced shows the area that was burned during each specific fire incident (Figure 8). The histograms of the fire risk map for the whole island and the area burned are presented separately.

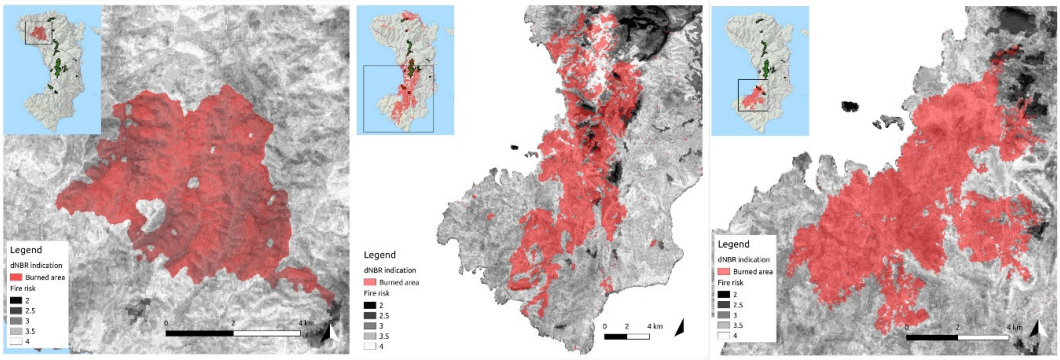

Figure 8. The burned area estimated from the dNBR of the dual Landsat-8 OLI images for the fires in 2007 (left), 2012 (middle), and 2016 (right) laid over the fire risk map produced from the multi-criteria model proposed.

3. Results and Discussion

The final fire risk map is in good agreement with all the individual layers considered. The value ranges for the individual factors taken into account were determined for the specific characteristics of the study area. The factor that was assigned the highest weight was land cover, which relates to the abundance of fuel available for fire ignition and propagation. This parameter attributes a high level of risk in areas already identified as high risk for fire combustion (Table S1), which was based on the CLC land use/land cover classification. An example of the good agreement between the fire risk map and the actual burned area is shown in the forested areas in the central axis of the island.

The actual fires recorded in 2007, 2012 and 2016 were located in areas that were categorized as 'high' and 'very high risk' by the GIS model. This agreement becomes apparent in Figure 9, where the histograms of the fire risk map of the whole island and the area corresponding to the burn scars are presented. The pixels of burned areas follow a distribution, which in general corresponds well to the higher fire risk index in the final map produced in the GIS proposed; it is essential to note that low fire risk values (<3) are absent from the burned areas while they cover a considerable percentage of the whole island distribution.

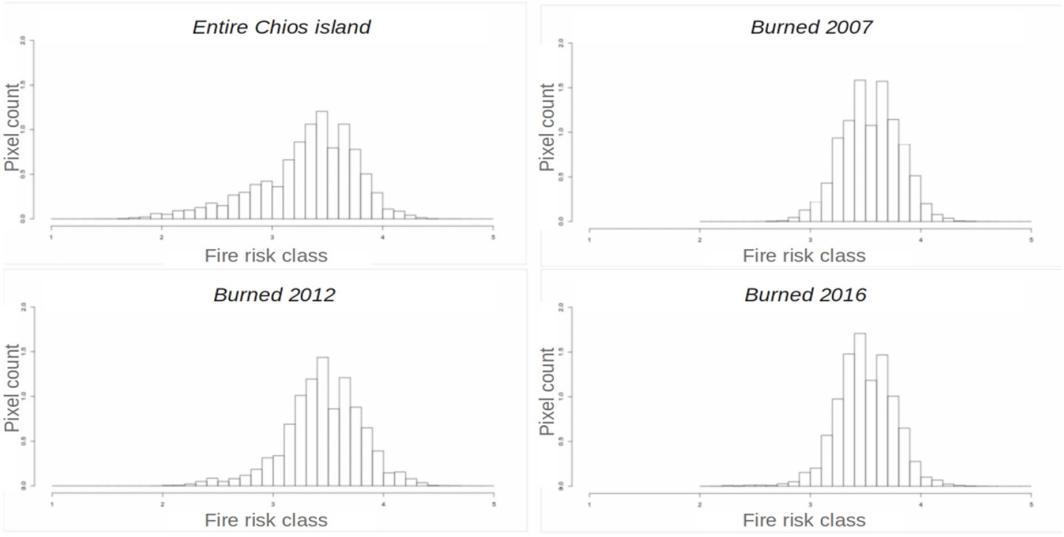

Figure 9. Histograms of the fire risk map for the entire island (upper left) and the pixels contributing to the area burned from the fires in 2007 (upper right), 2012 (lower left) and 2016 (lower right).

The areas burned by the 2007, 2012 and 2016 fires generally have southern and western aspects that receive a relatively high solar illumination (Figure 9). A clear correlation between the number of fire outbreaks and the proximity to a road was also observed. In addition, there is good agreement with the elevation parameter. Chios is generally a mountainous island, and the flat areas are primarily found in the southern and eastern parts, while the highest peaks are in the Northern part of the island (Pelineo Mt, St, Ilias top reaching 1297 m).

An interesting observation concerning the fire ignition in the year 2016 is the prevailing weather conditions. On 25 July 2016, when Greece declared a state of emergency on Chios, the fire that broke out was fanned by windy conditions. The wind direction was northerly, with a minimum speed of 11 km/hr and a maximum speed of 23 km/hr (data from an adjacent meteorological station of the island—Mytilini National Meteorological Service station). This supports the argument of an ignition in the north part of the burn scar and the spread of the fire towards the south. This argument supports the proposed GIS's prediction for 'very high' risk factor at the location of the fire ignition. The air temperatures for the specific day were T minimum = 23 °C and T maximum = 34 °C; and the minimum, maximum and average relative humidity were 17%, 48% and 34%, respectively. This specific weather

profile, a hot and dry day with relatively strong winds during the warm season of the year and well into that season (hot and dry for a prolonged period), favors the spread of a fire [67].

The fires that devastated the island in 2012 lasted for 5 days (18–22 August). The same meteorological station gave the following data for 18 August 2012: The minimum temperature was 24 °C while the maximum was 29 °C, and the minimum and maximum relative humidities were 45% and 65%, respectively (reasonably high relative humidity), with an average of 56%. The wind speed ranged from a minimum of 19 km/hr to a maximum of 28 km/hr. The values of these parameters were similar for the following days as well. Even though the weather profile was somewhat different, meaning not very high temperatures and not very low humidity, there was a devastating fire. This fact could highlight the importance of further assessment of the static component in fire risk analysis that has been performed in this study.

For all the years tested, the assessment was satisfactory since the majority of actual fires were located in areas that were identified as high and very high-risk zones, which has also been documented in other similar studies [26,40,68–71]. The overall performance of the approach proposed in the current paper and the respective GIS (highlighting the flexibility to be developed based on geospatial information solely) showed that it has the potential to contribute to the efforts of forest fire prevention as a useful and user-friendly tool for forest fire management.

Weather is the most dynamic factor determining fire danger as it affects FMC—particularly of the dead fuel and to an extent determines wind direction [72,73]. This is the reason why most of the operational fire risk assessment/forecasting systems are primarily based on meteorological data measurements and/or predictions. As mentioned earlier, Greece currently uses such a system. However, the volume of meteorological data necessary is large, and their calibration requires thorough ground data collections. The meteorological variables used are obtained from weather stations that provide information for point locations. Thus, it is necessary to apply interpolation techniques to create a spatially continuous variable, yet this approach can yield different outputs from different interpolation algorithms based on the same input variables [74]. In situations where the weather stations are more than 20 km away, interpolation methods may produce poor results [75]. In this study, a remote sensing approach was used to account for the meteorological factors, resulting in an estimate of the change in canopy water content over time. In addition, we integrated NDII, a liquid-water spectral index that is a robust indicator of water availability in the soil for use by vegetation.

The final map produced in the study is not a forecast or outlook model tied to a particular day or season. It is instead intended for longer-term strategic wildfire planning and associated fuel management, something which is currently lacking not only in the specific area but across Greece. When paired with the specific spatial data depicting resources and assets in the area, our method showed that it could successfully approximate relative wildfire risk. The proposed GIS can be used for other areas as well, since the respective datasets are available, at no actual or associated costs of data and license acquisition. When the aforementioned fire risk assessment tool is applied in a new environment, it should be adjusted and evaluated for the meteorological conditions and the vegetation cover of the new area. This approach could, for example, be easily adjusted to other regions of Greece but also across the Mediterranean region since there is some degree of similarity in the region's landscapes and climate.

Reliable fire risk forecasting constitutes one of the most important components of wildfire management and public safety. Maps like the one produced in the current study can be useful for civil protection agencies and associated authorities, in that groups involved could set up an appropriate firefighting infrastructure for the areas more prone to fire occurrence. Like those produced in the current study, maps will prove helpful to the local land managers, as this type of data would enable the groups involved to set up an appropriate firefighting infrastructure for the areas more prone to fire occurrence. For example, in the case of Chios, fire watchtowers could be created in the areas that have been identified as vulnerable and there could be an improved planning of the main subsidiary roads and other access routes. Our approach could also assist in creating a reliable system to efficiently fight

small and large occurring fires by identifying areas where wildfires are likely to occur. Services and communities may prioritize areas of concern and guide decision-making efforts accordingly.

The current intended to create an easily used fire risk assessment GIS based on publicly available geospatial data. The lack of other types of data, for example, meteorological data (that would have to be requested and/or purchased from services, or do not exist in an organized manner) is an important constraint. Although fires are such an essential and consistent challenge for Greece, the data that is readily available for fire warning is certainly coarse by current standards and not relevant to the area/s topographic and physiographic characteristics.

4. Conclusions

Large forested areas are burned every year in the Mediterranean, leading to widespread environmental and economic damage. The valuable assets at risk include the wildland environment and our collective cultural and historical heritage and justify the development of targeted measures such as 1. preventing wildfire when possible, and 2. managing wildfires when and where ignitions occur. In these two respects, integrated solutions with a broad scope should be promoted to ensure the protection of these important natural and cultural assets.

The assessment of forest and shrubland fire impact is unquestionably an essential consideration for the improved management of wildland resources. Additionally, any efforts aimed at fire prevention, through the identification of high-risk areas, is also of crucial importance. This paper presented the design and creation of a multi-criteria GIS model for the production of a fire risk assessment tool and its application on the island of Chios, an area of exceptional ecological and cultural value. The proposed approach was tested comparing the fire maps produced (for the years 2007, 2012 and 2016) with our GIS-based results. A significant advantage of the method proposed is the use of a validated layer of information for the 'vegetation' factor, thus avoiding possible errors associated with produced classifications. Other factors that have an effect on wildland fire were calculated, namely a proxy to FMC, illumination, topography, and proximity to human infrastructure. The relative importance between the factors was examined and determined and a map that provides information about the areas that are at a higher wildfire risk was produced. To validate the methodology proposed, actual historical fire occurrence maps were employed and compared to the fire hazard zone area derived from the prediction model. The results were in agreement as the actual fire spots were located in areas that are identified as high and very high-risk zones as in similar studies.

The added valued of the framework proposed is that it relies on data that is freely and readily available, overcoming the difficulties associated with the provision of other types of data that need to be requested or purchased. At the same time, the products are user-friendly and save the potential users from the burden of trying to understand complex parameters or technical details that go beyond their level of experience. This advantage may allow local communities to have up-to-date and accurate information and act accordingly to prepare effective fire management strategies. The authors plan to test the methodology proposed for other areas of the country that have been repeatedly affected by wildfires and investigate the robustness and the predictive performance of the GIS model.

Supplementary Materials: The following are available online at http://www.mdpi.com/2220-9964/9/9/516/s1, Table S1: Corine Land Cover classes present in the scene and the categorical value of LULC score attributed according to the CLC type.

Author Contributions: Nektaria Adaktylou: conceptualization, methodology, original draft preparation, reviewing and editing; Dimitris Stratoulias: conceptualization, data curation, investigation, visualization, original draft preparation, reviewing and editing; Rick Landenberger: conceptualization, funding acquisition, reviewing and proof-reading. All authors have read and agreed to the published version of the manuscript.

Funding: This research received no external funding.

Acknowledgments: The authors would like to express their gratitude to the 4 anonymous reviewers for their constructive comments.

Conflicts of Interest: The authors declare no conflict of interest.

References

1. FAO. *Global Forest Resources Assessment 2005: Progress Towards Sustainable Forest Management*; Food and Agriculture Organization of the United Nations: Rome, Italy, 2006.
2. Houghton, R.A.; Ramakrishna, K. A review of national emissions inventories from select non-annex I countries: Implications for counting sources and sinks of carbon. *Annu. Rev. Energy Environ.* **1999**, *24*, 571–605. [CrossRef]
3. Morancho, A.B. A hedonic valuation of urban green areas. *Landsc. Urban. Plan.* **2003**, *66*, 35–41. [CrossRef]
4. Nuthammachot, N.; Phairuang, W.; Stratoulias, D. Estimation of carbon emission in the ex-mega rice project, indonesia based on sar satellite images. *Appl. Ecol. Environ. Res.* **2019**, *17*, 2489–2499. [CrossRef]
5. Alexandrian, D.; Esnault, F.; Calabri, G. Forest fires in the Mediterranean area. In Proceedings of the FAO Meeting on Public Policies Affecting Forest Fires, Italy, Rome, 28–30 October 1998; pp. 28–30.
6. Balch, J.K.; Bradley, B.A.; Abatzoglou, J.T.; Nagy, R.C.; Fusco, E.J.; Mahood, A.L. Human-started wildfires expand the fire niche across the United States. *Proc. Natl. Acad. Sci. USA* **2017**, *114*, 2946–2951. [CrossRef]
7. Roy, P.S. Forest Fire and Degradation Assessment Using Satellite Remote Sensing and Geographic Information System. In *Satellite Remote Sensing and GIS Applications in Agricultural Meteorology I*; WMO: Geneva, Switzerland, 2003; Volume 361.
8. Maheras, G. Forests fires in Greece. The Analysis of the Phenomenon Affecting both Natural Human Environment The Role of Sustainable Development in Controlling Fire Effects. Ph.D. Thesis, Lund University, Lund, Sweden, 2002.
9. Rundel, P.; Arroyo, M.T.; Cowling, R.M.; Keeley, J.E.; Lamont, B.B.; Vargas, P. Mediterranean biomes: Evolution of their vegetation, floras, and climate. *Annu. Rev. Ecol. Evol. Syst.* **2016**, *47*, 383–407. [CrossRef]
10. European Environment Agency. 2019. Available online: https://www.eea.europa.eu/data-and-maps/indicators/forest-fire-danger-3/assessment (accessed on 19 August 2020).
11. Khabarov, N.; Krasovskii, A.; Obersteiner, M.; Swart, R.; Dosio, A.; San-Miguel-Ayanz, J.; Durrant, T.; Camia, A.; Migliavacca, M. Forest fires and adaptation options in Europe. *Reg. Environ. Chang.* **2014**, *16*, 21–30. [CrossRef]
12. Vélez, R. High intensity forest fires in the Mediterranean basin: Natural and socio-economic causes. *Disaster Manag.* **1993**, *5*, 16–21.
13. Dimitriou, A.; Mantakas, G.; Kouvelis, S. An Analysis of Key Issues that Underlie Forest Fires and Shape Subsequent Fire Management Strategies in 12 Countries in the Mediterranean Basin. In *Final Report Prepared by Alcyon for WWF Mediterranean Programme Office and IUCN*; WWF project 9Z0731.01; WWF: Gland, Switzerland, 2001.
14. Birch, D.S.; Morgan, P.; Kolden, C.A.; Abatzoglou, J.T.; Dillon, G.K.; Hudak, A.T.; Smith, A.M.S. Vegetation, topography and daily weather influenced burn severity in central Idaho and western Montana forests. *Ecosphere* **2015**, *6*, art17. [CrossRef]
15. Estes, B.L.; Knapp, E.E.; Skinner, C.N.; Miller, J.D.; Preisler, H.K. Factors influencing fire severity under moderate burning conditions in the Klamath Mountains, Northern California, USA. *Ecosphere* **2017**, *8*, e01794. [CrossRef]
16. Dillon, G.K.; Holden, Z.A.; Morgan, P.; Crimmins, M.A.; Heyerdahl, E.K.; Luce, C.H. Both topography and climate affected forest and woodland burn severity in two regions of the western US, 1984 to 2006. *Ecosphere* **2011**, *2*, art130. [CrossRef]
17. Fang, L.; Yang, J.; Zu, J.; Li, G.; Zhang, J. Quantifying influences and relative importance of fire weather, topography, and vegetation on fire size and fire severity in a Chinese boreal forest landscape. *Ecol. Manag.* **2015**, *356*, 2–12. [CrossRef]
18. Viedma, O.; Quesada, J.; Torres, I.; De Santis, A.; Moreno, J.M. Fire severity in a large fire in a pinus pinaster forest is highly predictable from burning conditions, stand structure, and topography. *Ecosystems* **2014**, *18*, 237–250. [CrossRef]
19. Hardy, C.C. Wildland fire hazard and risk: Problems, definitions, and context. *Ecol. Manag.* **2005**, *211*, 73–82. [CrossRef]
20. Keane, R.E.; Drury, S.A.; Karau, E.C.; Hessburg, P.F.; Reynolds, K.M. A method for mapping fire hazard and risk across multiple scales and its application in fire management. *Ecol. Model.* **2010**, *221*, 2–18. [CrossRef]

21. Chuvieco, E.; Aguado, I.; Yebra, M.; Nieto, H.; Salas, J.; Martín, M.P.; Vilar, L.; Martínez-Vega, J.; Martín, S.; Ibarra, P.; et al. Development of a framework for fire risk assessment using remote sensing and geographic information system technologies. *Ecol. Model.* **2010**, *221*, 46–58. [CrossRef]
22. Chuvieco, E.; Deshayes, M.; Stach, N.; Cocero, D.; Riaño, D. Short-Term Fire Risk: Foliage Moisture Content Estimation from Satellite Data. In *Remote Sensing of Large Wildfires*; Springer: Berlin/Heidelberg, Germany, 1999; pp. 17–38.
23. Marzano, R.; Bovio, G.; Guglielmet, E.; Jappiot, M.; Lampin, C.; Dauriac, F.; Deshayes, M.; Salas, J.; Aguado, I.; Martínez, J.; et al. *Common Methods for Mapping the Wildland Fire Danger*; EUFIRELAB: Euro-Mediterranean Wildland Fire Laboratory, a "wall-less" Laboratory for Wildland Fire Sciences and Technologies in the Euro-Mediterranean Region. Deliverable D-08-05; HAL Inrea: Bangalore, India, 2004.
24. Lozano, F.J.; Suarez-Seoane, S.; Kelly, M.; Luis, E. A multi-scale approach for modeling fire occurrence probability using satellite data and classification trees: A case study in a mountainous Mediterranean region. *Remote. Sens. Environ.* **2008**, *112*, 708–719. [CrossRef]
25. Chuvieco, E.; Salas, J. Mapping the spatial distribution of forest fire danger using GIS. *Int. J. Geogr. Inf. Syst.* **1996**, *10*, 333–345. [CrossRef]
26. Jaiswal, R.K.; Mukherjee, S.; Raju, K.D.; Saxena, R. Forest fire risk zone mapping from satellite imagery and GIS. *Int. J. Appl. Earth Obs. Geoinf.* **2002**, *4*, 1–10. [CrossRef]
27. Chuvieco, E.; Riaño, D.; Aguado, I.; Cocero, D. Estimation of fuel moisture content from multitemporal analysis of Landsat Thematic Mapper reflectance data: Applications in fire danger assessment. *Int. J. Remote. Sens.* **2002**, *23*, 2145–2162. [CrossRef]
28. Viegas, D.X.; Bovio, G.; Ferreira, A.D.; Nosenzo, A.; Sol, B. Comparative study of various methods of fire danger evaluation in southern Europe. *Int. J. Wildland Fire* **1999**, *9*, 235–246. [CrossRef]
29. Fang, L.; Yang, J.; White, M.; Liu, Z. Predicting potential fire severity using vegetation, topography and surface moisture availability in a eurasian boreal forest landscape. *Forests* **2018**, *9*, 130. [CrossRef]
30. Yakubu, I.; Mireku-Gyimah, D.; Duker, A.A. Review of methods for modelling forest fire risk and hazard. *Afr. J. Env. Sci. Technol.* **2015**, *9*, 155–165. [CrossRef]
31. Desbois, N.; Deshayes, M.; Beudoin, A. *In Protocol for Fuel Moisture Content Measurements. A Review of Remote Rensing Methods for the Study of Large Wildland Fires*; Chuvieco, E., Ed.; Universidad de Alcalá: Alcalá de Henares, Spain, 1997; pp. 61–72.
32. Verbesselt, J.; Fleck, S.; Coppin, P. Estimation of fuel moisture content towards fire risk assessment: A review. *For. Fire Res. Wildland Fire Saf.* **2002**, *55*.
33. Sriwongsitanon, N.; Gao, H.; Savenije, H.; Maekan, E.; Saengsawang, S.; Thianpopirug, S. Comparing the normalized difference infrared index (NDII) with root zone storage in a lumped conceptual model. *Hydrol. Earth Syst. Sci.* **2016**, *20*, 3361–3377. [CrossRef]
34. Hardisky, M.; Klemas, V.; Smart, R.M. The influences of soil salinity, growth form, and leaf moisture on the spectral reflectance of spartina alterniflora canopies. *Photogramm. Eng. Remote Sens.* **1983**, *49*, 77–83.
35. Sağlam, B.; Bilgili, E.; Durmaz, B.D.; Kadiogullari, A.I.; Kucuk, O. Spatio-temporal analysis of forest fire risk and danger using landsat imagery. *Sensors* **2008**, *8*, 3970–3987. [CrossRef] [PubMed]
36. Setiawan, I.; Mahmud, A.; Mansor, S.; Shariff, A.; Nuruddin, A. GIS-grid-based and multi-criteria analysis for identifying and mapping peat swamp forest fire hazard in Pahang, Malaysia. *Disaster Prev. Manag. Int. J.* **2004**, *13*, 379–386. [CrossRef]
37. Darmawan, M.; Masamu, A.; Satoshi, T. Forest fire hazard model using remote sensing and geographic information systems: Toward understanding of land and forest degradation in lowland areas of East Kalimantan, Indonesia. In Proceedings of the 22nd Asian Conference on Remote Sensing, Singapore, 5–9 November 2001.
38. Sowmya, S.V.; Somashekar, R.K. Application of remote sensing and geographical information system in mapping forest fire risk zone at Bhadra wildlife sanctuary, India. *J. Environ. Boil.* **2010**, *31*, 969.
39. Ajin, R.; Jacob, M.; Menon, A.; Vinod, P. Forest Fire Risk Analysis Using Geo-Information Technology: A Study of Peppara Wildlife Sanctuary, Thiruvananthapuram, Kerala, India. In Proceedings of the 2nd Disaster, Risk and Vulnerability Conference, Trivandrum, India, 24–26 April 2014.
40. Vinod, P.G.; Ajin, R.S.; Jacob, M.K. RS and GIS based spatial mapping of forest fires in Wayanad wildlife sanctuary, Wayanad, North Kerala, India. *Int. J. Earth Sci. Eng.* **2016**, *9*, 498–502.

41. Nuthammachot, N.; Stratoulias, D. A GIS- and AHP-based approach to map fire risk: A case study of Kuan Kreng peat swamp forest, Thailand. *Geocarto Int.* **2019**, 1–14. [CrossRef]
42. Adaktylou, N.E.; Stratoulias, D. A GIS Multi-criteria approach for forest fire risk assessment: A case study for chios, Greece. In Proceedings of the AGU Fall Meeting, Washington, DC, USA, 10–14 December 2018.
43. Wirawan, N. Factors Promoting the Spread of Fire. 2000. Available online: http://www.nzdl.org/gsdlmod?e=d-00000-00---off-0hdl--00-0----0-10-0---0---0direct-10---4-------0-0l--11-en-50---20-help---00-0-1-00-0-0-11-1-0utfZz-8-00-0-0-11-10-0utfZz-8-10&cl=CL1.16&d=HASH40ec50fb1eb727e72e746a.8.7.4&gt=1 (accessed on 19 August 2020).
44. Mansor, S.; Abu Shariah, M.; Billa, L.; Setiawan, I.; Jabar, F. Spatial technology for natural risk management. *Disaster Prev. Manag. Int. J.* **2004**, *13*, 364–373. [CrossRef]
45. Chuvieco, E.; Congalton, R.G. Application of remote sensing and geographic information systems to forest fire hazard mapping. *Remote. Sens. Environ.* **1989**, *29*, 147–159. [CrossRef]
46. Jo, M.H. The development of forest fire forecasting system using internet GIS and satellite remote sensing. In Proceedings of the 21st Asian Conference on Remote Sensing, Singapore, 5–9 November 2001.
47. Ierapetritis, D. The Geography of the chios mastic trade from the 17th through to the 19th century. *Ethnobot. Res. Appl.* **2010**, *8*, 153–167. [CrossRef]
48. Abraham, E.; Kyriazopoulos, A.; Korakis, G.; Parissi, Z.; Chouvardas, D. Wild fire effects on floristic diversity in three thermo-mediterranean vegetation types in a small islet of eastern Aegean sea. In Proceedings of the EGU General Assembly, Vienna, Austria, 27 April–2 May 2014.
49. European Commission NATURA 2000. 2008. Available online: http://ec.europa.eu/environment/nature/natura2000/index_en.htm (accessed on 19 August 2020).
50. Keeley, J.E. Fire in Mediterranean climate ecosystems—A comparative overview. *Isr. J. Ecol. Evol.* **2012**, *58*, 123–135.
51. Turco, M.; Rosa-Cánovas, J.J.; Bedia, J.; Jerez, S.; Montávez, J.P.; Llasat, M.C.; Provenzale, A. Exacerbated fires in Mediterranean Europe due to anthropogenic warming projected with non-stationary climate-fire models. *Nat. Commun.* **2018**, *9*, 3821. [CrossRef]
52. UCAR/NCAR. Wildfires, Weather & Climate. 2010. Available online: https://news.ucar.edu/1437/wildfires-weather-climate (accessed on 19 August 2020).
53. Hellenic Statistical Authority. Population-Housing Census. 2011. Available online: http://www.statistics.gr/en/2011-census-pop-hous (accessed on 28 February 2019).
54. Keeley, J.E.; Bond, W.J.; Bradstock, R.A.; Pausas, J.G.; Rundel, P.W. *Fire in Mediterranean Ecosystems*; Cambridge University Press (CUP): Cambridge, UK, 2011.
55. Wright, J.; Lillesand, T.M.; Kiefer, R.W. Remote sensing and image interpretation. *Geogr. J.* **1980**, *146*, 448. [CrossRef]
56. Knight, J.; Gerbig, J.; Whitman, Z. Forest fire Threat Analysis in Crowsnest Pass, AB. 2003. Available online: https://ibis.geog.ubc.ca/courses/geob370/students/class06/fire/mce.html (accessed on 8 February 2017).
57. Robin, J.-G.; Carrega, P.; Fox, D.M. Modelling fire ignition in the Alpes-Maritimes department, France. *Ecol. Manag.* **2006**, *234*, S135. [CrossRef]
58. Gigović, L.; Jakovljević, G.; Sekulovic, D.; Regodić, M. GIS multi-criteria analysis for identifying and mapping forest fire hazard: Nevesinje, Bosnia and Herzegovina. *Teh. Vjesn. Tech. Gaz.* **2018**, *25*, 891–897. [CrossRef]
59. Saaty, T.L. A scaling method for priorities in hierarchical structures. *J. Math. Psychol.* **1977**, *15*, 234–281. [CrossRef]
60. Zadeh, L. Probability measures of fuzzy events. *J. Math. Anal. Appl.* **1968**, *23*, 421–427. [CrossRef]
61. Yu, P.L. A class of solutions for group decision problems. *Manag. Sci.* **1973**, *19*, 936–946. [CrossRef]
62. Zanter, K. *LANDSAT 8 (L8) Data Users Handbook (LSDS-1574 Version 5.0)*; United States Geological Survey: Sioux Falls, SC, USA, 2019.
63. Key, C.H.; Benson, N.C. Measuring and remote sensing of burn severity. In Proceedings of the Joint Fire Science Conference and Workshop: Crossing the Millennium: Integrating Spatial Technologies and Ecological Principles for a New Age in Fire Management, Boise, ID, USA, 15–17 June 1999.
64. Kontoes, C.; Poilvé, H.; Florsch, G.; Keramitsoglou, I.; Paralikidis, S. A comparative analysis of a fixed thresholding vs. a classification tree approach for operational burn scar detection and mapping. *Int. J. Appl. Earth Obs. Geoinf.* **2009**, *11*, 299–316. [CrossRef]

65. Veraverbeke, S.; Lhermitte, S.; Verstraeten, W.W.; Goossens, R. The temporal dimension of differenced normalized burn ratio (dNBR) fire/burn severity studies: The case of the large 2007 Peloponnese wildfires in Greece. *Remote. Sens. Environ.* **2010**, *114*, 2548–2563. [CrossRef]
66. Stratoulias, D. Burn Scar Mapping in Attica, Greece using the dNBR (differenced Normalised Burn Ratio) Index on Landsat TM/ETM+ Satellite Imagery. Master's Thesis, The University of Edinburgh, Edinburgh, UK, 2010.
67. Mitsopoulos, I.; Chrysafi, I.; Bountis, D.; Mallinis, G. Assessment of factors driving high fire severity potential and classification in a Mediterranean pine ecosystem. *J. Environ. Manag.* **2019**, *235*, 266–275. [CrossRef]
68. Nuthammachot, N.; Stratoulias, D. The synergistic use of AHP and GIS to assess factors driving forest fire potential in a peat swamp forest in Thailand. *Environ. Monit. Assess.* **2020**, In press.
69. Nuthammachot, N.; Stratoulias, D. Synergistic use of AHP and GIS for mapping forest fire risk in Hua Sai district, Thailand. *Environ. Dev. Sustain.* **2020**, In press.
70. Taibi, B.E.; Dridi, H.; Bouhata, R. Cartographie de la susceptibilité des incendies de forêt à I'aide de données de télédétection, des analyses SIG et AHP (étude de cas de Souhan, Algérie). *Int. J. Innov. Appl. Stud.* **2020**, *28*, 885–894.
71. Gülçin, D.; Deniz, B. Remote sensing and GIS-based forest fire risk zone mapping: The case of Manisa, Turkey. *Turk. J. Türkiye Orman. Derg.* **2020**, *21*, 15–24. [CrossRef]
72. Jolly, W.M.; Cochrane, M.A.; Freeborn, P.H.; Holden, Z.A.; Brown, T.J.; Williamson, G.J.; Bowman, D.M.J.S. Climate-induced variations in global wildfire danger from 1979 to 2013. *Nat. Commun.* **2015**, *6*, 7537. [CrossRef]
73. Torres, F.T.P.; Romeiro, J.M.N.; Santos, A.C.D.A.; Neto, R.R.D.O.; Lima, G.S.; Santos, A. Fire danger index efficiency as a function of fuel moisture and fire behavior. *Sci. Total. Environ.* **2018**, *631*, 1304–1310. [CrossRef]
74. Chowdhury, E.H.; Hassan, Q.K. Operational perspective of remote sensing-based forest fire danger forecasting systems. *IsprsJ. Photogramm. Remote. Sens.* **2015**, *104*, 224–236. [CrossRef]
75. Han, K.-S.; A Viau, A.; Anctil, F. High-resolution forest fire weather index computations using satellite remote sensing. *Can. J. Res.* **2003**, *33*, 1134–1143. [CrossRef]